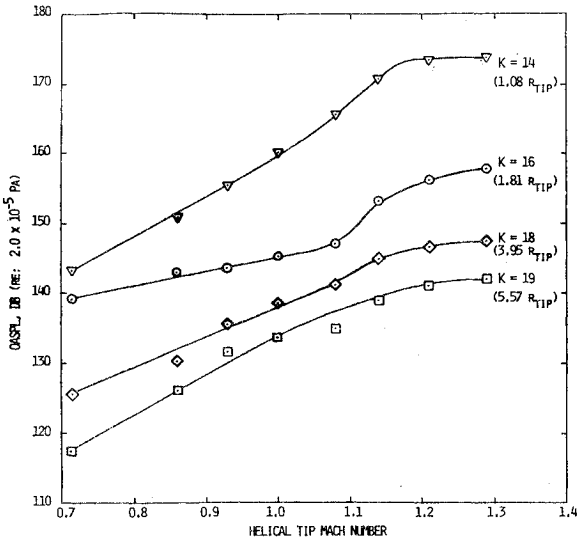

Fig. 3 Variation of OASPL with helical tip Mach number at $J=25$ (disk plane) at four radial locations.

Table 2 Comparison of predicted SPL levels with experimental data from Dittmar et al.[6,7]

Helical tip Mach number	Position 2[a]		Postion 5[b]	
	Experiment	Prediction	Experiment	Prediction
0.863	129.4	130	133.8	136.4
1.00	140.7	138.5	141.2	141.9
1.07	141.8	141	143.9	143.9
1.14	138.7	144	143.2	148.1
1.21	139.4	145	143.5	149.8

[a] $r=3.93R_{tip}$. [b] $r=2.95R_{tip}$.

and the SPL of the kth harmonic of the blade passing frequency is expressed as

$$\mathrm{SPL}_k = 10 \log_{10}[(a_k^2 + b_k^2)/(\sqrt{2}P_{ref})]^2 \quad (4)$$

Results and Discussion

The analysis procedure outlined above was applied to the eight cases shown in Table 1 for four points in the near field as indicated in Fig. 1. It may be noted that all of the points are located in the high-resolution area of the computational grid system, since the relatively coarse grid outside of this region yielded highly unreliable results in terms of OASPL. Likewise, the OASPL results at points located far from the propeller blade were not acceptable due to the relatively large influence of the numerical damping and boundary conditions.

Applying this method to the radial location of $1.82R_{tip}$ for a helical tip Mach number of 1.21, the calculated acoustic pressure-time history and spectral content is shown in Fig. 2. As noted, the acoustic time history is well behaved and the spectral content shows the proper decrease as the harmonic number increases. The OASPL, as calculated by this method, is shown in Fig. 3 as a function of helical tip Mach number and radial location at a fixed axial position in the propeller disk plane. As noted in Table 2, the theoretical predicted OASPL values compare well with the experimental noise quantities of Dittmar et al.[6,7] up to a helical tip Mach number of 1.07 at two microphone locations in the acoustic field of the propeller disk plane. It is postulated that very close to the propeller blade tip ($K=14$, $r=1.08R_{tip}$), the OASPL values first show a linear increase with helical tip Mach number, followed by a constant OASPL value. The influence of the shock wave system in the vicinity of the blade tip ($K=16$, 18; $r=1.81$, $3.95R_{tip}$) then becomes more pronounced, resulting in a sharp increase of the OASPL at a helical tip Mach number of approximately 1.1. As the point of calculation moves farther away from the blade tip, the influence of the shock wave system decreases where at $r=5.57R_{tip}$ ($K=19$), the OASPL curve shows the typical linear dependence on helical tip Mach number followed by a constant OASPL value.

Conclusions

The acoustic calculation method in this Note has been shown to be useful in the determination of acoustic near-field sound pressure level and frequency spectra for a range of operating conditions of the SR-3 propfan, yielding values that are comparable to experiment. Several areas have been suggested in which further study is needed and are currently under investigation. These include the effect of numerical damping, dependence of the acoustic values on the computational grid, and determination of the far-field acoustic characteristics.

Acknowledgment

This work was supported by NASA Lewis Research Center Grant NAG 3-354.

References

[1]Ffowcs Williams, J. E. and Hawkings, D. L., "Sound Generated by Turbulence and Surfaces in Arbitrary Motion," *Philosophical Transactions of the Royal Society of London*, Vol. A264, 1969.

[2]Lighthill, M. J., "On Sound Generation Aerodynamically: I. General Theory," *Proceeding of the Royal Society of London*, Vol. A221, 1952.

[3]Lighthill, M. J., "On Sound Generation Aerodynamically: II. Turbulence as a Source of Sound," *Proceedings of the Royal Society of London*, Vol. A222, 1954.

[4]Farassat, F., "Linear Acoustic Formulas for Calculation of Rotating Blade Noise," *AIAA Journal*, Vol. 19, Sept. 1981, pp. 1122-1130.

[5]Bober, L. J., Chaussee, D. S., and Kutler, P., "Prediction of High Speed Propeller Flow Fields Using a Three-Dimensional Euler Analysis," NASA TM 83065, 1983 (also AIAA Paper 83-0188).

[6]Dittmar, J. H., Jeracki, R. J., and Blaha, B. J., "Tone Noise of Three Supersonic Helical Tip Speed Propellers in a Wind Tunnel," NASA TM 79167, 1979.

[7]Dittmar, J. H. and Jeracki, R. J., "Additional Noise Data on the SR-3 Propeller," NASA TM 81736, 1981.

Constraints of the Structural Modal Synthesis

Jon-Shen Fuh* and Shyi-Yaung Chen*
Kaman Aerospace Corporation
Bloomfield, Connecticut

Structural Modal Synthesis

THE modal synthesis method has been a most active topic in structural dynamics since publication of Hurty's original paper.[1] In this method, a complex structure is treated as an assemblage of components, and modes of the structure are approximated by synthesizing component modes. To ensure that the components will act as a single structure, the geometric compatibility and/or force equilibrium conditions are imposed on the component inter-

Received Aug. 21, 1985; revision received Nov. 20, 1985.

*Senior Research Engineer. Member AIAA.

faces. The importance of component modes selected for efficiency of the synthesis method is obvious and has been thoroughly studied.[1-8] Along this line, various procedures using fixed,[1] free,[2,3] and hybrid[4,5] interfacial modes, among others,[6] were proposed. The effects of mode truncation and error compensations were also investigated.[7,8] Based on the Rayleigh-Ritz approach, modal synthesis leads to[8]

$$M\ddot{x}+Kx=A^T\lambda \tag{1}$$

subject to

$$Ax=0 \tag{2}$$

where λ is a vector containing unknown Lagrange multipliers, and M and K are mass and stiffness matrices of the structural system formulated by assembling component mass and stiffness matrices while leaving all components uncoupled. Thus, generalized coordinates, x, are not all independent; dependence of the coordinates is given in Eq. (2) which states compatibility and/or equilibrium conditions. Let A be a matrix of $m\times n$, $m<n$, where m is the number of constrained equations and n the number of generalized coordinates. When there are redundancies in the constrained equations, r (the rank of A) is less than m. Equations (1) and (2) constitute a constrained linear system.

Constrained System and Orthogonal Complement

The zero-eigenvalues theorem (Walton and Steeves[9]) is quite popular in dealing with constrained problems.[8,10] Equations (1) and (2) can be coupled by introducing to the system an orthogonal complement of A, which is composed of independent eigenvectors associated with the zero eigenvalues of A^TA. For a complex structure, n may be large, even major model reduction performed in the component level. Thus, solving eigenproblems of an $n\times n$ matrix A^TA is very inefficient, if not intractable.

The following concepts are reviewed before introducing a simple, powerful technique for constrained systems. The null space of A, $N(A)$, is the set containing all vectors y such that $Ay=0$. A basis for $N(A)$ has independent vectors which span the null space and, therefore, is an orthogonal complement of A. Apparently, the basis of $N(A)$ is not unique.

For any matrix A, there exists a pair of orthogonal matrices (P,Q) such that[11,12]

$$PAQ=\begin{pmatrix} U & V \\ 0 & 0 \end{pmatrix} \tag{3}$$

in which U is a nonsingular upper triangular matrix of rank r, and P and Q are of the order m and n, respectively. This partitioned form can be obtained by using a Gauss elimination procedure or Householder transformation.[12] From the last equation

$$A=P^T\begin{pmatrix} U & V \\ 0 & 0 \end{pmatrix}Q^T \tag{4}$$

and a basis for $N(A)$

$$B=Q\begin{pmatrix} U^{-1}V \\ -I_{n-r} \end{pmatrix} \tag{5}$$

where the identity matrix I_{n-r} is of the order $n-r$. The inverse of an upper triangular U is easily solved. Therefore, systematic construction of an orthogonal complement of A (whose rank may be less than its row dimension) is straightforward by using the Gauss elimination or Householder transformation, since the permutation matrix Q is retrievable from well-developed subroutine packages. It is acknowledged that a similar formation of B in Eq. (5) appeared in Walton and Steeves' paper,[9] but was restricted to the case of A being full rank, i.e., $r=m$. Note that if the orthogonal matrix P is replaced by an elementary row operation matrix, then $U=I_r$ and the matrix inversion in Eq. (5) is waived. However, the total computational expenses for these two options are essentially the same.

Formulation of Coupled System Equation

Let $x=Bs$. The transformation reduces the number of generalized coordinates from n to $n-r$. Premultiplying Eq. (1) by B^T and noting that $AB=0$ results in the coupled system equation

$$M^*\ddot{s}+K^*s=0 \tag{6}$$

where

$$M^*=B^TMB, \quad K^*=B^TKB$$

Modes of the structure are obtained from Eq. (6) and the transformation $x=Bs$.

Discussion

A stated advantage of using the zero-eigenvalues theorem is the relief of rank determination. However, considering numerical errors introduced specifically in large eigenproblems, a criterion (tolerance) is always needed to judge the number of zero-eigenvalues of A^TA. This task is no easier than setting a tolerance to determine the rank of A, especially when n is much larger than r. The present approach invokes rank determination, as shown in Eq. (3). Accounting for numerical errors, the lower right submatrix in the partitioned form of Eq. (3) is no longer null (in contrast with the exact computation in the equation), but a matrix W with elements of small values. In this case, the rank is determined from the value of each element (or a matrix norm) compared to a specified tolerance. In practical situations, many strategies[12] are used satisfactorily for this purpose. For procedures based on a Gauss elimination method (with the matrix scaled), it is convenient to use complete or partial pivoting[13] with linear dependence checks. For the Householder transformation based procedures,[6] use of pivoting and comparison of the greatest norm in the columns of W is usually sufficient. In the successive elimination (Gauss) or transformation (Householder) processes, if the value of each element of W suddenly drops to the same order as the significant number of digits of the computer, then W should be treated as a null matrix. On the other hand, a gradual decrease in the values of elements of W may indicate that the matrix A is ill-posed. Under this extreme condition, applying the suggested strategies (and zero-eigenvalues theorem) may not accurately determine the rank, and subjective judgment is required. More discussion of related computation and application details are presented in Refs. 12 and 14.

The basis of $N(A)$ given in Eq. (5) (and any other orthogonal complement) is not a unique set. Nevertheless, this does not affect the unique solution of x, as B is no more than a transformation between two sets of coordinates.

Extension of the present approach to the formulation of modal synthesis of a damped structural system is straightforward. It is also expected that this procedure can be applied to dynamics of large constrained multibody systems (spacecrafts, robots, and biomechanical systems, etc.) where automated numerical formulations and computational efficiency in real-time environments are concerns.

References

[1]Hurty, W. C., "Dynamic Analysis of Structural Systems Using Component Modes," *AIAA Journal*, Vol. 3, April 1965, pp. 678-685.

[2]Hou, S. N., "Review of Modal Synthesis Techniques and a New Approach," *Shock and Vibration Bulletin*, Vol. 40, Pt. 4, Dec. 1969, pp. 25-30.

[3]Benfield, W. A. and Hruda, R. F., "Vibration Analysis of Structures by Component Mode Substitution," *AIAA Journal*, Vol. 9, July 1971, pp. 1255-1261.

[4]MacNeal, R. H., "A Hybrid Method of Component Mode Synthesis," *Computers and Structures*, Vol. 1, Dec. 1971, pp. 581-601.
[5]Rubin, S., "Improved Component Mode Representation," *AIAA Journal*, Vol. 13, Aug. 1975, pp. 995-1006.
[6]Meirovitch, L. and Hale, A. L., "On the Substructure Synthesis Method," *AIAA Journal*, Vol. 19, July 1981, pp. 940-947.
[7]Hintz, R. M., "Analytical Methods in Component Modal Synthesis," *AIAA Journal*, Vol. 13, Aug. 1975, pp. 1007-1016.
[8]Kuang, J. H. and Tsuei, Y. G., "A More General Method of Substructure Mode Synthesis for Dynamic Analysis," *AIAA Journal*, Vol. 23, April 1985, pp. 618-623.
[9]Walton, W. C. Jr. and Steeves, E. C., "A New Matrix Theorem and Its Application for Establishing Independent Coordinates for Complex Dynamic Systems with Constraints," NASA TR R-326, 1969.
[10]Kamman, J. W. and Huston, R. L., "Dynamics of Constrained Multibody Systems," *Journal of Applied Mechanics*, ASME, Vol. 51, Dec. 1984, pp. 899-903.
[11]Ben-Israel, A. and Greville, T.N.E., *Generalized Inverse, Theory and Applications*, John Wiley & Sons, New York, 1974.
[12]Noble, B., "Methods for Computing the Moore-Penrose Generalized Inverse and Related Matters," *Generalized Inverses and Applications*, edited by M. Z. Nashed, Academic Press, New York, 1976, pp. 245-301.
[13]Greene, B. E., Jones, R. E., McLay, R. W., and Strome, D. R., "On the Application of Generalized Variational Principles in the Finite Element Method," AIAA Paper 68-290, 1968.
[14]Chen, S. Y. and Fuh, J. S., "Reply by Authors to J. A. Brandon," *AIAA Journal*, Vol. 23, Nov. 1985, pp. 1840-1841.

Toward a Consistent Plate Theory

A. V. Krishna Murty*
Indian Institute of Science, Bangalore, India

In Ref. 1 a beam theory has been given, avoiding some of the traditional contradictions normally tolerated in the elementary- and Timoshenko-type shear deformation beam theories. In this theory a cubic variation of the direct stress and parabolic variation shear stress across the depth of the beam have been considered. Numerical results pertaining to a tip-loaded cantilevered beam indicate that the theory of Ref. 1 is capable of giving stress distributions corresponding to Timoshenko-type shear deformation theory in regions where transverse shear effect is significant, and elementary-theory-type stress distributions in regions where transverse shear effect is insignificant, with smooth transition patterns in between. In this Note, the corresponding theory for flexure of plates is presented.

Figure 1 shows a typical plate subjected to a dynamic load $f(x,y,t)$. Following Ref. 1, the displacement field is chosen in the form

$$w(x,y) = w_b(x,y) + w_s(x,y)$$
$$u(x,y,z) = -zw_{b,x} - p(z)\phi(x,y)$$
$$v(x,y,z) = -zw_{b,y} - p(z)\psi(x,y) \tag{1}$$

where w_b is the partial deflection due to bending and w_s the partial deflection due to shear. ϕ and ψ represent the nonclassical in-plane displacement distribution

$$p = z(1 - 4z^2/3h^2) \tag{2}$$

The strain-displacement relations are

$$\epsilon_x = \frac{\partial u}{\partial x}, \quad \epsilon_{xy} = \frac{\partial u}{\partial y} + \frac{\partial v}{\partial x}, \quad \epsilon_y = \frac{\partial v}{\partial y}$$
$$\epsilon_{xz} = \frac{\partial u}{\partial z} + \frac{\partial w}{\partial x}, \quad \epsilon_z = 0, \quad \epsilon_{yz} = \frac{\partial v}{\partial z} + \frac{\partial w}{\partial y} \tag{3}$$

and the stress-strain relations are

$$\sigma_x = \lambda(\epsilon_x + \mu\epsilon_y), \qquad \sigma_y = \lambda(\epsilon_y + \mu\epsilon_x)$$
$$\sigma_{ij} = \lambda g \epsilon_{ij}; \quad i \neq j, \quad i,j = x,y,z \tag{4}$$

where

$$\lambda = \frac{E(1-\nu)}{(1+\nu)(1-2\nu)} \quad \text{and} \quad \mu = \frac{\nu}{1-\nu}$$

which correspond to $\epsilon_z = 0$ and $\sigma_z \neq 0$. However, if one assumes ϵ_z and $\sigma_z = 0$, as in the case of the classical thin-plate theory, the corresponding values will be $\lambda = E/(1-\nu^2)$ and $\mu = \nu$. In either case,

$$g = G/\lambda$$

where G is the shear modulus, E Young's modulus, and ν Poisson's ratio.

Utilizing Hamilton's principle, the equations of motion may be obtained as

$$\lambda[I\nabla^4 w_b + C\nabla^2(\phi_{,x} + \psi_{,y})] - \rho I\nabla^2 \ddot{w}_b + \rho C(\ddot{\phi}_{,x} + \ddot{\psi}_{,y}) + \rho h[\ddot{w}_b + \ddot{w}_s] = f(x,y,t)$$
$$\lambda g[h\nabla^2 w_s - c(\phi_{,x} + \psi_{,y}) - \rho h[\ddot{w}_s + \ddot{w}_b] = f(x,y,t)$$
$$\lambda[D(\phi_{,xx} + (\mu+g)\psi_{,xy}) + g\phi_{,yy} + C\nabla^2 w_{b,x} + gcw_{s,y} - gd\phi] - \rho[C\ddot{w}_{b,x} + D\ddot{\phi}] = 0$$
$$\lambda[D(\psi_{,yy} + (\mu+g)\phi_{,xy} + g\psi_{,xx}) + C\nabla^2 w_{b,y} + gcw_{s,x} - gd\psi] - \rho[C\ddot{w}_{b,y} + D\ddot{\psi}] = 0 \tag{5}$$

where the overdot indicates derivation with time and the $,x$ or $,y$ subscript indicates derivation with respect to the variable indicated and

$$\nabla^2 = \frac{\partial^2}{\partial x^2} + \frac{\partial^2}{\partial y^2}$$

$$I = h^3/12, \quad C = h^3/15, \quad D = 19h^3/315, \quad c = 2h/3, \quad d = 8h/15 \tag{6}$$

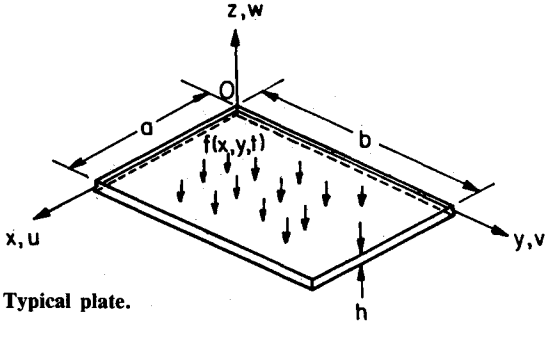

Fig. 1 Typical plate.

Received Feb. 19, 1985; revision received Aug. 14, 1985.

*Professor, Department of Aerospace Engineering. Member AIAA.